ECS Journal of Solid State
Science and Technology

Comparison of 10 MeV Neutron Irradiation Effects on NiO/Ga_2O_3 Heterojunction Rectifiers and Ni/Au/Ga_2O_3 Schottky Rectifiers

To cite this article: Jian-Sian Li *et al* 2023 *ECS J. Solid State Sci. Technol.* **12** 075004

ECS Journal of Solid State Science and Technology, 2023 **12** 075004

Comparison of 10 MeV Neutron Irradiation Effects on NiO/Ga_2O_3 Heterojunction Rectifiers and $Ni/Au/Ga_2O_3$ Schottky Rectifiers

Jian-Sian Li,[1] Xinyi Xia,[1] Chao-Ching Chiang,[1] Hsiao-Hsuan Wan,[1] Fan Ren,[1] Jihyun Kim,[2] and S. J. Pearton[3,z]

[1] *Department of Chemical Engineering, University of Florida, Gainesville, FL, 32606, United States of America*
[2] *School of Chemical and Biological Engineering, Seoul National University, Seoul 08826, Republic of Korea*
[3] *Department of Materials Science and Engineering, University of Florida, Gainesville, FL, 32606, United States of America*

Neutrons generated through charge-exchange ^9Be (p; n^i) ^9Be reactions, with energies ranging from 0–33 MeV and an average energy of ~9.8 MeV were used to irradiate conventional Schottky Ga_2O_3 rectifiers and NiO/Ga_2O_3 p-n heterojunction rectifiers to fluences of 1.1–2.2 × 10^{14} cm^{-2}. The breakdown voltage was improved after irradiation for the Schottky rectifiers but was highly degraded for their NiO/Ga_2O_3 counterparts. This may be a result of extended defect zones within the NiO. After irradiation, the switching characteristics were degraded and irradiated samples of both types could not survive switching above 0.7 A or 400 V, whereas reference samples were robust to 1 A and 1 kV. The carrier removal rate in both types of devices was ~45 cm^{-1}. The forward currents and on-state resistances were only slightly degraded by neutron irradiation.
 [DOI: 10.1149/2162-8777/ace54e]

Manuscript submitted December 14, 2022; revised manuscript received June 12, 2023. Published July 17, 2023.

There is significant recent interest in Ga_2O_3-based rectifiers for power inversion applications because of their lower switching losses and higher breakdown voltages compared to SiC and GaN.[1–12] A recent advance has also come from the use of p-NiO/n-Ga_2O_3 heterojunction rectifiers to overcome the absence of a native p-type doping capability in Ga_2O_3.[13–33] While excellent dc and switching performance has been reported from these devices, there is little information on their response to radiation. One of the most common forms of radiation encountered by semiconductor devices is neutron irradiation.[34–37] Neutrons create primary knock-on displaced atoms in semiconductors, which produce trap states in the bandgap and degrade the electrical properties. The main mechanism for producing these displaced atoms is elastic and inelastic collisions between the incoming neutron and nuclei in the crystalline semiconductor.[37] If a high enough energy is transferred, there may also be further displacements, producing a cascade of defects. There is also the possibility of atomic displacement due to neutron capture interaction and related nuclear reactions. These defects cause trap states mostly created by non-ionizing energy-loss (NIEL) processes,[38,39] which generate primary defects by the initial particle interaction and by the cascade generation due to nucleus recoil, and secondary defects caused by the diffusion of the primary point defects.[40] For fast neutrons which create large recoil cascades, carrier removal is by disordered regions in which the Fermi level in the core is pinned.

There are numerous applications where neutron exposure to neutron fluxes may occur, including nuclear reactors or simply terrestrial neutron showers due to interactions of high-energy primary cosmic rays with gases in the upper atmosphere.[36,37] This flux increases at lower altitude due to a higher number of cosmic ray–gas and neutron–gas interactions, The maximum flux is ~1 n $cm^{-2}s$ at 20 km altitude. The terrestrial neutron flux decreases at lower altitudes altitude due to scattering and decreased cosmic ray energy. The energy per cm^3 deposited through atomic displacements by neutrons is characterized by the spectral fluence $\phi(E)$ in units of n/cm^2 MeV.[36,37]

The amount of non-ionizing energy loss varies greatly for different types of radiation, as shown in Fig. 1 for β-Ga_2O_3. Here we have calculated the NIEL for a typical fast heavy ion, Au, as well as protons, electrons, alpha particles and neutrons.[38] While neutrons are the least damaging from this regard, their ubiquity in the environment means there is a need to understand their effects on Ga_2O_3-based devices.[41–45]

In this paper, we report a comparison of 10 MeV neutron irradiation of NiO/Ga_2O_3 heterojunction rectifiers with conventional Schottky Ga_2O_3 rectifiers. We find no significant difference in the response of the two types of rectifiers to neutron irradiation, and a high degree of robustness against neutron damage in both cases.

Experimental

The common epitaxial layer structure for both Schottky and heterojunction rectifiers consisted of 8 μm thick halide vapor phase epitaxy (HVPE) layer (2 × 10^{16} cm^{-3}) grown by (001) n^+ β-Ga_2O_3 substrate (Novel Crystal Technology, Japan). A full-area backside Ti/Au Ohmic contact was deposited by e-beam evaporation and annealed at 550 °C for 60 s under N_2.[30] For the heterojunction rectifiers we deposited a bilayer NiO structure by magnetron sputtering (3 mTorr, 150 W, 13.56 MHz). The carrier concentration in the bilayer (10 nm/10 nm) structure was controlled by the Ar/O_2 ratio during sputtering at levels of 2 × 10^{18}–3 × 10^{19} cm^{-3}. The structures were completed with Ni/Au (200–1000 μm diameter) deposited onto either the NiO layer in the case of the heterojunction devices or the bare Ga_2O_3 in the case of the Schottky rectifiers. Figure 2 shows schematics of both device structures.

The neutron irradiation was performed at the Korea Institute of Radiological and Medical Science with a 45 MeV MC-50 cyclotron. 35 MeV protons colliding with beryllium elements generated neutrons by nuclear reactions. The beam passes through two Al degrader films before hitting the Be target. Production of energetic neutrons is dominated by charge-exchange ^9Be (p; n^i) ^9Be reactions. The proton to neutron generation ratio was approximately 8200:1. The average energy of the generated neutrons was 9.8 MeV, as shown in the spectrum of Fig. 3. The devices were irradiated for 2 or 4 h with the total fluence of 1.1 × 10^{14} or 2.2 × 10^{14} cm^{-2} of neutrons at room temperature. The rectifiers were not under bias during the neutron irradiation.

The current-voltage (I–V) characteristics were recorded with a Tektronix 370-A curve tracer, 371-B curve tracer and Agilent 4156C was used for forward and reverse current measurements. The capacitance-voltage (C–V) measurements were made on the parameter analyzer. The reverse recovery was measured on a pulse generator.

Results and Discussion

The C–V data was plotted in the form C^{-2}–V in Fig. 4 to extract the carrier concentration before and after the neutron

[z]E-mail: spear@mse.ufl.edu

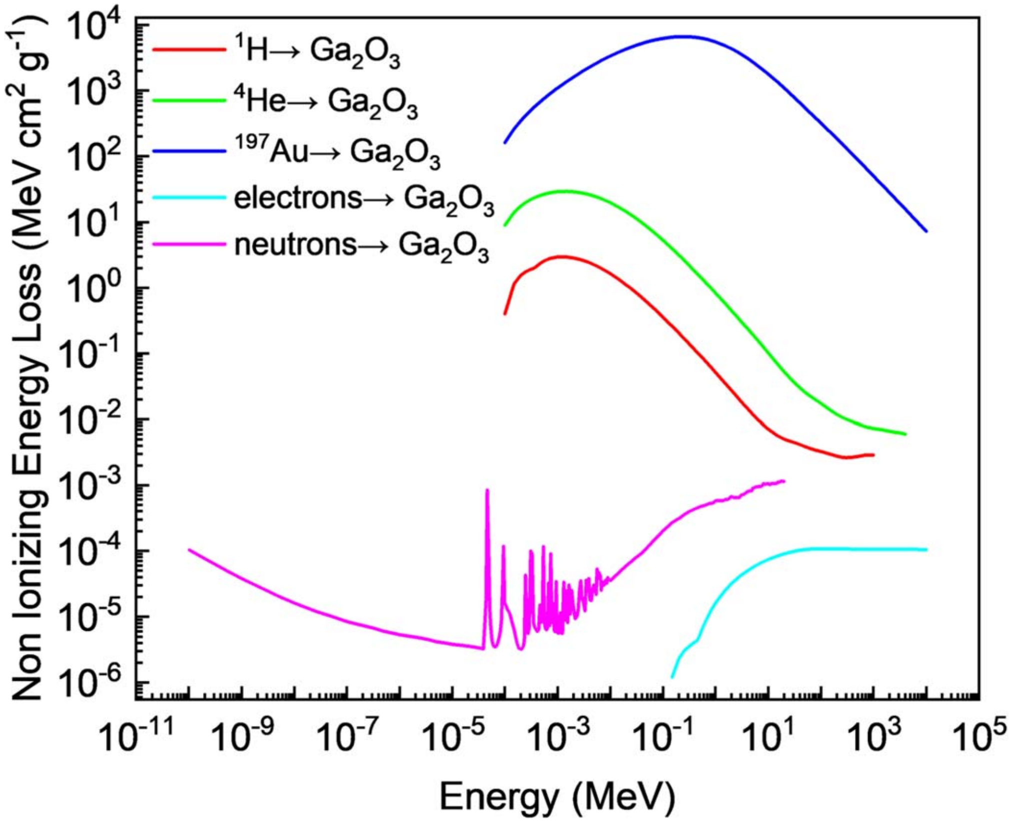

Figure 1. NIEL loss as a function of energy for protons, alpha particles, a typical heavy ion (Au), electrons and neutrons in Ga_2O_3.

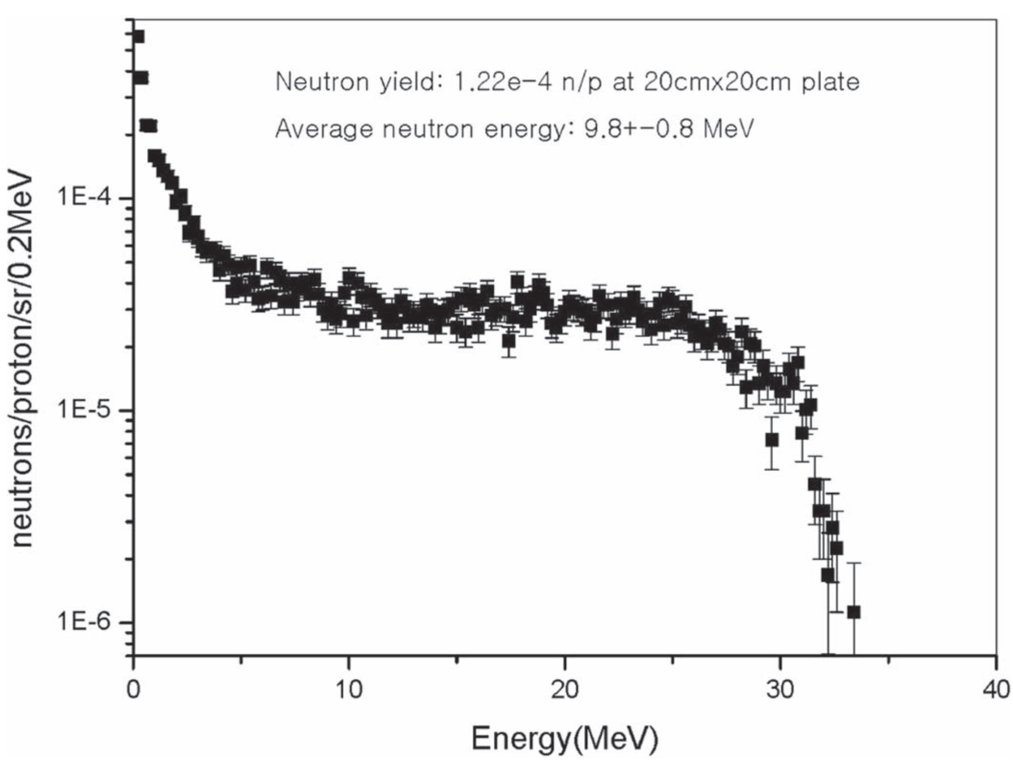

Figure 2. Neutron/proton yield as a function of energy from the irradiation source used in these experiments.

irradiation of both types of devices. These are expected to be similar since the depletion in the both the p-n heterojunctions and the Schottky rectifier will be in the n-Ga_2O_3. As tabulated in Table I, the carrier concentration is slightly reduced after neutron irradiation, with an approximate carrier removal rate, R_C, defined by[44,45]

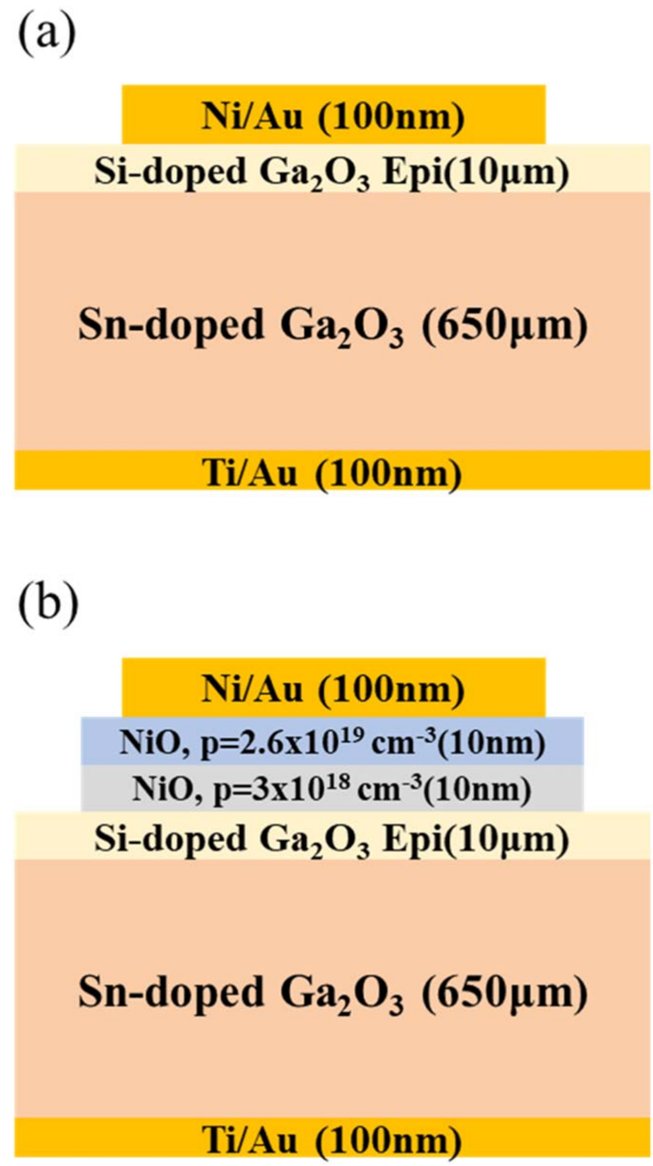

Figure 3. Schematic of the (a) Ga_2O_3 Schottky rectifiers and (b) NiO/Ga_2O_3 heterojunction rectifiers.

Table I. Summary of changes in electrical properties of Schottky and heterojunction NiO/Ga_2O_3 rectifiers as a result of neutron irradiation at two different doses. N_D is the drift region carrier concentration, W_n is the depletion width and V_{bi} is the built-in bias.

Sample	N_D (Ga_2O_3) (cm^{-3})	W_n (nm)	V_{bi} (V)
Ga_2O_3 ref	2.1×10^{16}	236	1.05
1.1×10^{14}	1.1×10^{16}	382	1.43
2.2×10^{14}	1.05×10^{16}	397	1.49
NiO/Ga_2O_3 ref	2.1×10^{16}	240	2.09
1.1×10^{14}	2.0×10^{16}	247	2.7
2.2×10^{14}	1.5×10^{16}	290	253

$$R_C = (n_{s0} - n_s)/\Phi$$

where Φ is the neutron fluence, n_{s0} is initial carrier concentration, and n_s is the irradiated carrier concentration. The R_C value was

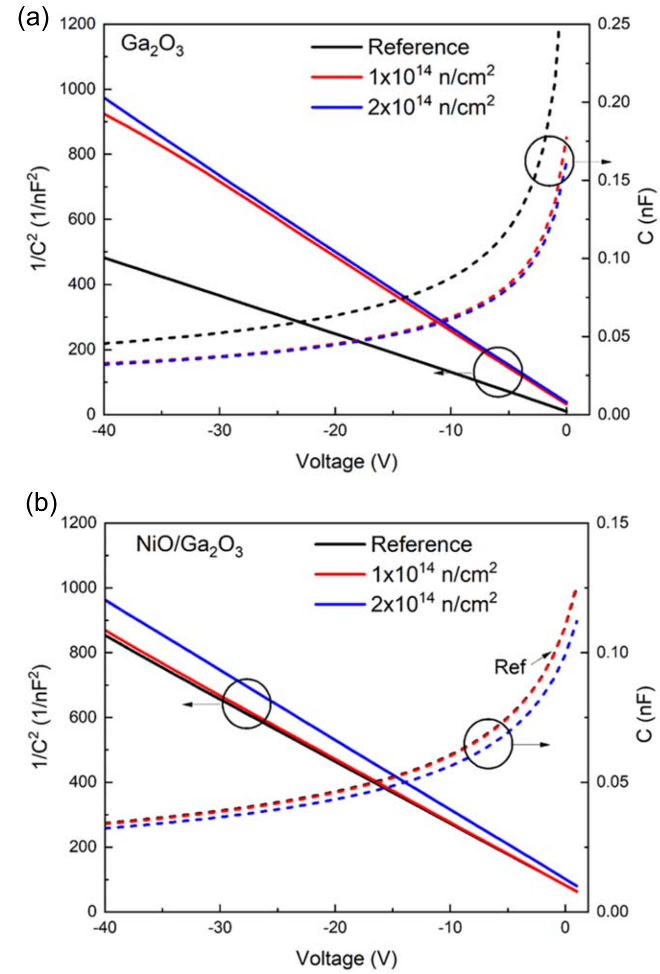

Figure 4. C^{-2}-V characteristics from (top) Schottky Ga_2O_3 rectifiers and (bottom) NiO/Ga_2O_3 heterojunction rectifiers before and after neutron irradiation.

$\sim$45 cm^{-1}, which is broadly consistent with reported values for neutrons with similar or lower energies, given the large uncertainties in some cases of this parameter. Farzana et al.[40] reported a removal rate of $\sim$51 cm^{-1} for n-Ga_2O_3 irradiated with reactor neutrons with energy spread $\sim$1–20 MeV. Lee et al.[45] reported a removal rate of $\sim$480 cm^{-1} for neutrons of average energy 4.2 MeV from a ^{241}Am-Be source, with energy spread 1–11 MeV. The removal rates in β-Ga_2O_3 for neutrons are on par with those reported for n-GaN and n-SiC.[40,44–46]

Figure 5 shows the forward I–V characteristics from the two types of devices. There are only minor reductions in forward current and increase in on-state resistance, $R_{ON,}$ because of the neutron irradiation. Table I also shows only relatively minor increases in the built-in voltage of the Schotttky and p-n junctions. This is not too unexpected since the NiO is highly conducting and should not be affected much by the neutrons,[30] which have a long mean free path in Ga_2O_3 of >10 cm. This is obviously much larger than the total sample thickness of the samples. The scattering cross section of neutrons in NiO is <0.5 cm^{-1} indicates the average number of interactions per neutron is of order 2×10^5 reactions/cm^{-2} for the NiO region of the rectifier structure 2000 times higher for the depletion region at the highest dose condition.

Figure 6 shows the reverse I–V characteristics at low biases, with little change in reverse current for either type of rectifier. However, there was a significant effect on reverse breakdown voltage, as shown in Fig. 7 and tabulated in Table I. The first thing to note is the

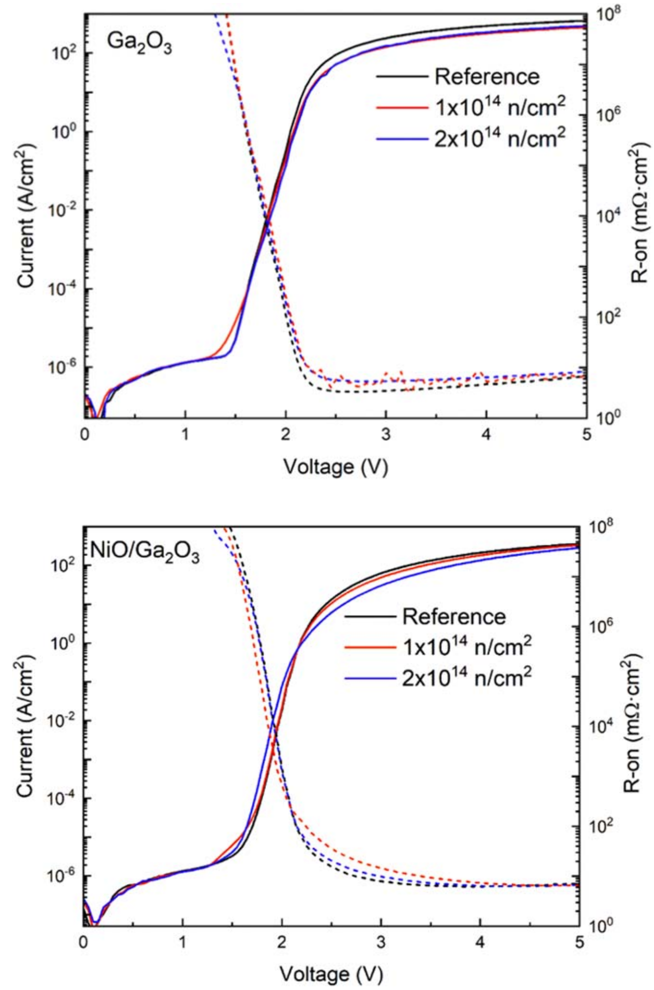

Figure 5. Forward I-V and on-state resistance characteristics from (top) Schottky Ga_2O_3 rectifiers and (bottom) NiO/Ga_2O_3 heterojunction rectifiers before and after neutron irradiation.

Table II. Summary of switching performance of Schottky and heterojunction NiO/Ga_2O_3 rectifiers before and after neutron irradiation. T_{rr} is the reverse recovery time, I_{rr} the reverse recovery current, dI/dT is the rate of current during the switching and I_F the forward current at 10 V.

Sample	T_{rr} (ns)	I_{rr} (mA)	dI/dt (A/μs)	I_F (mA)
Ga_2O_3 ref	29.7	−50	4.5	122
1.1×10^{14}	28.1	−47	4.4	109
2.2×10^{14}	26.4	−41	4.2	109
NiO/Ga_2O_3 ref	27.6	−45	4.2	97
1.1×10^{14}	27.6	−46	4.1	91
2.2×10^{14}	27.8	−46	3.9	84

large increase in V_B when the NiO is used as the cathode contact relative to the Schottky metal on the same epitaxial layer structure. This has been noted by numerous authors and emphasizes also that the NiO provides excellent edge termination. The V_B increased after irradiation for the Schottky rectifiers, from 884 V for the reference to 1.2 kV for the highest neutron dose. By sharp contrast, the V_B for the NiO/Ga_2O_3 showed a sharp decrease upon neutron irradiation, from 3.96 kV in the reference to 1.32 kV in the highest dose device. The increase in the conventional Schottky rectifier might be ascribed to

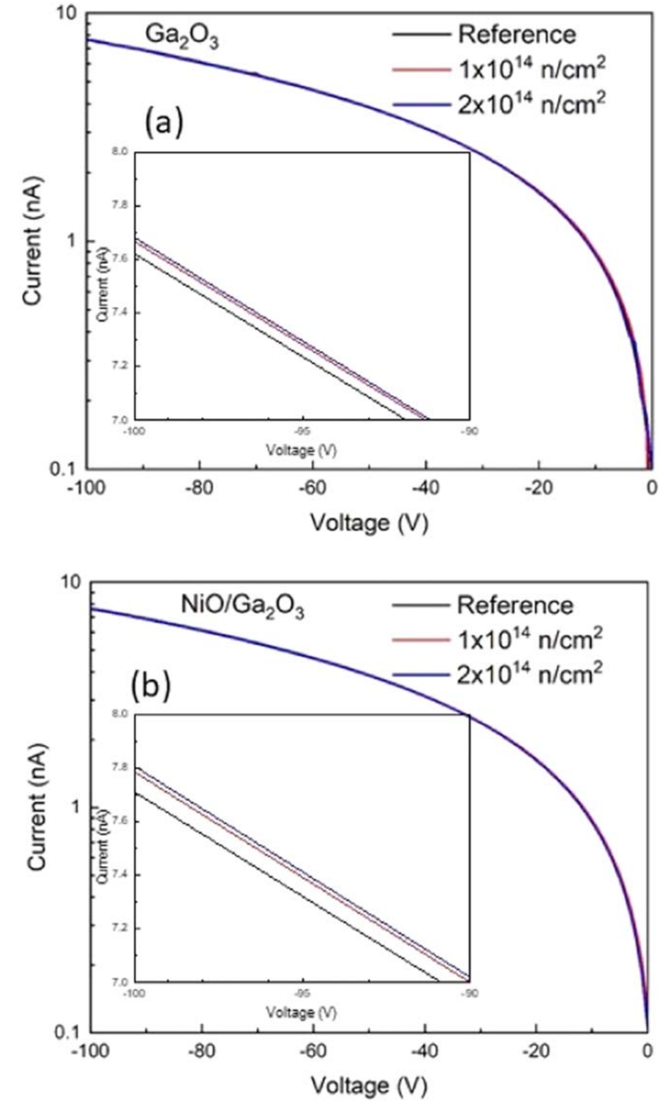

Figure 6. Reverse I-V characteristics at low bias from (top) Schottky Ga_2O_3 rectifiers and (bottom) NiO/Ga_2O_3 heterojunction rectifiers before and after neutron irradiation. The insets show the differences arising from the neutron irradiation.

the small decease in effective carrier concentration in the drift region. If this where the only effect present, then the V_B of the NiO devices should also increase. The large degradation in V_B in those devices indicated there is a change in the NiO itself, since the breakdown voltages trend back towards those of the Schottky rectifiers. Note that the reverse current is suppressed compared to the reference up to the point of breakdown. This may indicate creation of disordered regions (Gossick zones)[43,47–49] within the NiO because of neutron irradiation. We plan to examine single layers of NiO by high resolution electron microscopy to try to directly observe if such damage zones are present.

Figure 8 shows the reverse recovery characteristics before and after neutron irradiation for both types of rectifiers. The measurement circuit condition was switching the bias from +10 to −10 V for a period of 10 μS (duty cycle 20%) and switching period of 50 μS. Table II summarizes the resultant reverse recovery time constants, T_{rr}, defined as the time required to reach 25% of the peak current, as well as the Irr and rate of change of current, dI/dt (A/μs). The changes in these parameters after irradiation are relatively small in all cases.

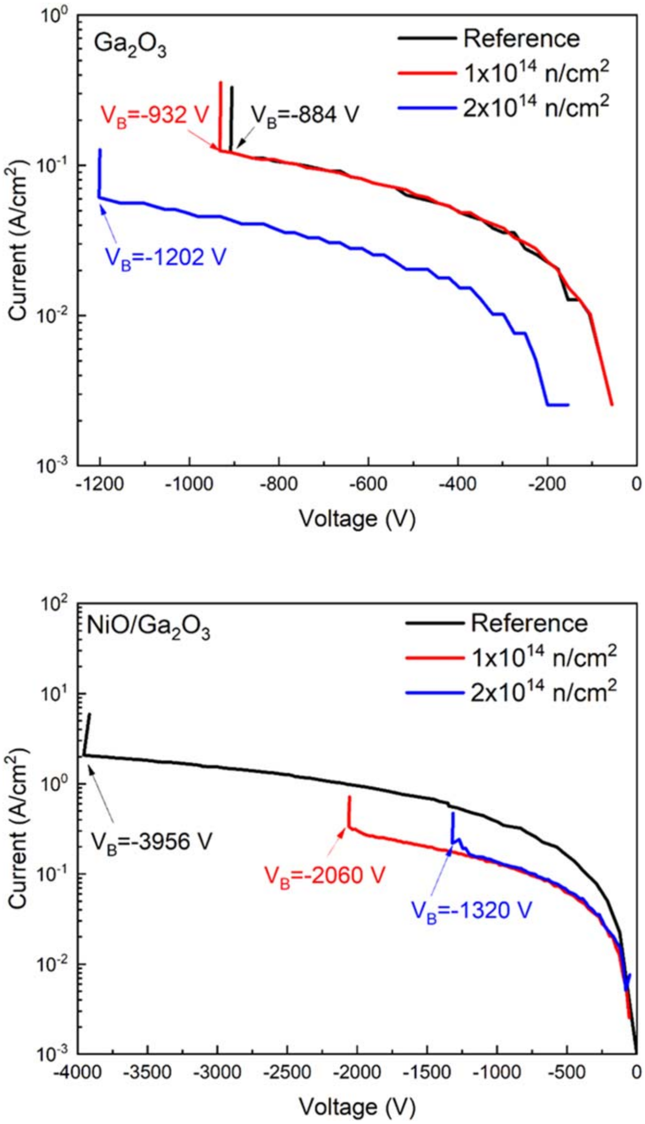

Figure 7. Reverse I-V characteristics from (top) Schottky Ga_2O_3 rectifiers and (bottom) NiO/Ga_2O_3 heterojunction rectifiers before and after neutron irradiation. The breakdown voltages are indicated in each case.

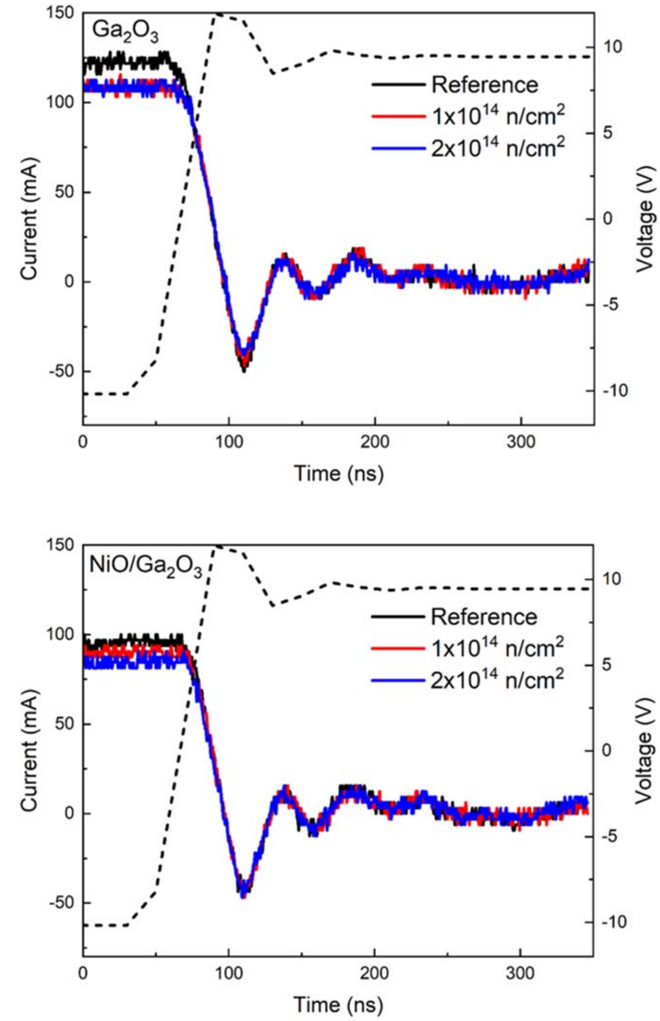

Figure 8. Switching characteristics from (top) Schottky Ga_2O_3 rectifiers and (bottom) NiO/Ga_2O_3 heterojunction rectifiers before and after neutron irradiation, measured under pulsed conditions (Period = 50 μS, Duty Cycle = 1 μS (20%) Power Supply = +10/−10 V.

Summary and Conclusions

In summary, a comparison of the effects of neutron irradiation on conventional Schottky Ga_2O_3 rectifiers and NiO/Ga_2O_3 p-n heterojunction rectifiers shows that neutron irradiation had contrasting effects on the reverse breakdown voltage of these devices. Neutron irradiation of Schottky and p-n heterojunction Ga_2O_3 rectifiers shows major differences in the effect on reverse breakdown voltage. In the case of conventional Schottky rectifiers, the reverse breakdown voltage increases with neutron dose, due to a decrease in the effective carrier concentration in the drift region.[49] By sharp contrast, NiO/Ga_2O_3 heterojunction rectifiers fabricated on the same epitaxial layer structures show significant decreases in reverse breakdown voltage because of the same neutron irradiations. There was little difference in the forward or low-bias reverse currents between the two structures and little significant change in reverse recovery characteristics. Additional characterization and simulations to support our hypothesis are planned to provide a more comprehensive understanding of the observed behavior. This will provide more insight into the potential implications of the observed differences in reverse breakdown voltage on the overall performance and reliability of the rectifiers, since these will affect considerations of device applications, limitations, and possible mitigation strategies to enhance the radiation hardness of the NiO/Ga_2O_3 heterojunction rectifiers. While the use of NiO to produce a p-n junction has a major beneficial effect on improving breakdown voltage in vertical geometry Ga_2O_3 rectifiers, it brings disadvantages in terms of the radiation hardness of the devices.

Acknowledgments

The work at UF was performed as part of Interaction of Ionizing Radiation with Matter University Research Alliance (IIRM-URA), sponsored by the Department of the Defense, Defense Threat Reduction Agency under award HDTRA1–20–2–0002. The content of the information does not necessarily reflect the position or the policy of the federal government, and no official endorsement should be inferred. The work at UF was also supported by NSF DMR 1856662 (James Edgar). The work in Korea was supported by the Korea Institute for Advancement of Technology (KIAT) (P0012451, The Competency Development Program for Industry Specialist), the National Research Foundation of Korea (2020M3H4A3081799) and the K-Sensor Development Program (RS-2022-00154729), funded by the Ministry of Trade, Industry and Energy (MOTIE, Korea).

Declarations

The authors have no conflicts to disclose.

ORCID

Jian-Sian Li https://orcid.org/0000-0002-2817-7612
Xinyi Xia https://orcid.org/0000-0002-8644-8599
Chao-Ching Chiang https://orcid.org/0000-0002-0447-8170
Hsiao-Hsuan Wan https://orcid.org/0000-0002-6986-8217
Jihyun Kim https://orcid.org/0000-0002-5634-8394
S. J. Pearton https://orcid.org/0000-0001-6498-1256

References

1. J. Yang, F. Ren, M. Tadjer, S. J. Pearton, and A. Kuramata, *AIP Adv.*, **8**, 055026 (2018).
2. W. Li, K. Nomoto, Z. Hu, D. Jena, and H. G. Xing, *IEEE Electr. Device L*, **41**, 107 (2020).
3. P. P. Sundaram, F. Alema, A. Osinsky, and S. J. Koester, *J. Vac. Sci. Technol. A*, **40**, 043211 (2022).
4. R. Sharma, M. Xian, C. Fares, M. E. Law, M. Tadjer, K. D. Hobart, F. Ren, and S. J. Pearton, *J. Vac. Sci. Technol. A*, **39**, 013406 (2021).
5. W. Li, D. Saraswat, Y. Long, K. Nomoto, D. Jena, and H. G. Xing, *Appl. Phys. Lett.*, **116**, 192101 (2020).
6. Y. Lv et al., *IEEE T Power Electr.*, **36**, 6179 (2021).
7. J. Yang et al., *Appl. Phys. Lett.*, **114**, 232106 (2019).
8. J. Yang, F. Ren, Y.-T. Chen, Y.-T. Liao, C.-W. Chang, J. Lin, M. J. Tadjer, S. J. Pearton, and A. Kuramata, *IEEE J. Electron Devi.*, **7**, 57 (2019).
9. T. Harada and A. Tsukazaki, *Appl. Phys. Lett.*, **116**, 232104 (2020).
10. C.-H. Lin et al., *IEEE Electr Device L.*, **40**, 1487 (2019).
11. W. Xiong et al., *IEEE Electr. Device L.*, **42**, 430 (2021).
12. S. J. Pearton, J. Yang, P. H. Cary, F. Ren, J. Kim, M. J. Tadjer, and M. A. Mastro, *Appl. Phys. Rev.*, **5**, 011301 (2018).
13. M. Xiao et al., *IEEE T. Power Electr.*, **36**, 8565 (2021).
14. X. Lu, X. Zhou, H. Jiang, K. Wei Ng, Z. Chen, Y. Pei, K. May Lau, and G. Wang, *IEEE Electr. Device L.*, **41**, 449 (2020).
15. C. Wang et al., *IEEE Electr. Device. L*, **42**, 485 (2021).
16. Q. Yan et al., *Appl. Phys. Lett.*, **118**, 122102 (2021).
17. H. H. Gong, X. H. Chen, Y. Xu, F.-F. Ren, S. L. Gu, and J. D. Ye, *Appl. Phys. Lett.*, **117**, 022104 (2020).
18. H. Gong et al., *IEEE T. Power Electr.*, **36**, 12213 (2021).
19. H. H. Gong et al., *Appl. Phys. Lett.*, **118**, 202102 (2021).
20. H. H. Gong, X. H. Chen, Y. Xu, Y. T. Chen, F. F. Ren, B. Liu, S. L. Gu, R. Zhang, and J. D. Ye, *IEEE T. Electron Dev.*, **67**, 3341 (2020).
21. W. Hao, Q. He, K. Zhou, G. Xu, W. Xiong, X. Zhou, G. Jian, C. Chen, X. Zhao, and S. Long, *Appl. Phys. Lett.*, **118**, 043501 (2021).
22. F. Zhou et al., *IEEE T. Power Electr.*, **37**, 1223 (2022).
23. Q. Yan, H. Gong, H. Zhou, J. Zhang, J. Ye, Z. Liu, C. Wang, X. Zheng, R. Zhang, and Y. Hao, *Appl. Phys. Lett.*, **120**, 092106 (2022).
24. J. Yang, F. Ren, M. Tadjer, S. J. Pearton, and A. Kuramata, *ECS J. Solid State SC.*, **7**, Q92 (2018).
25. P. Dong, J. Zhang, Q. Yan, Z. Liu, P. Ma, H. Zhou, and Y. Hao, *IEEE Electr. Device L.*, **43**, 765 (2022).
26. Y. Wang et al., *IEEE T Power Electron.*, **37**, 3743 (2022).
27. W. Li, D. Jena, and H. G. Xing, *J. Appl. Phys.*, **131**, 015702 (2022).
28. H. Sheoran, V. Kumar, and R. Singh, *ACS Appl. Electron. Mater.*, **4**, 2589 (2022).
29. M. Xian, C. Fares, F. Ren, B. P. Gila, Y.-T. Chen, Y.-T. Liao, M. Tadjer, and S. J. Pearton, *J. Vac. Sci. Technol. B*, **37**, 061201 (2019).
30. J.-S. Li, C.-C. Chiang, X. Xia, F. Ren, H. Kim, and S. J. Pearton, *Appl. Phys. Lett.*, **121**, 042105 (2022).
31. Y.-T. Chen, J. Yang, F. Ren, C.-W. Chang, J. Lin, S. J. Pearton, M. J. Tadjer, A. Kuramata, and Y.-T. Liao, *ECS J. Solid State SC.*, **8**, Q3229 (2019).
32. C. Liao et al., *IEEE Trans Electron. Dev.*, **69**, 5722 (2022).
33. J. Zhang et al., *Nature Comm.*, **13**, 3900 (2022).
34. J. F. Ziegler, *IBM J. Res. Develop.*, **42**, 117 (1998).
35. A. Akturk, J. M. McGarrity, N. Goldsman, D. Lichtenwalner, B. Hull, D. Grider, and R. Wilkins, *IEEE Trans. Nucl. Sci.*, **65**, 1248 (2018).
36. R. Campesato et al., "NIEL Dose Analysis on triple and single junction InGaP/GaAs/Ge solar cells irradiated with electrons, protons and neutrons." *Proceedings of the 2019 IEEE 46th Photovoltaic Specialist Conference (PVSC), June 16–21 (2019), Chicago (USA), Book Series: IEEE Photovoltaic Specialists Conference,* 2381 (2019).
37. C. Leroy and P. G. Rancoita, *Principles of Radiation Interaction in Matter and Detection* 4th ed.(World Scientific, Singapore) (2016), Screened Relativistic-NIEL Calculator Website, https://Sr-niel.org/index.php.
38. C. Leroy and P. G. Rancoita, *Rep. Prog. Phys.*, **70**, 493 (2007).
39. J. Kim, S. J. Pearton, C. Fares, J. Yang, F. Ren, S. Kim, and A. Y. Polyakov, *J. Mater. Chem. C*, **7**, 10 (2018).
40. E. Farzana, A. Mauze, J. B. Varley, T. E. Blue, J. S. Speck, A. R. Arehart, and S. A. Ringel, *APL Mater.*, **7**, 121102 (2019).
41. M. F. Chaiken and T. E. Blue, *IEEE Trans Nuclear Sci.*, **65**, 1147 (2018).
42. A. Y. Polyakov et al., *J. Phys. D: Appl. Phys.*, **53**, 274001 (2020).
43. S. J. Pearton et al., *ECS J. Solid State Sci. Technol.*, **10**, 055008 (2021).
44. X. Xia et al., *ECS J. Solid State Technol.*, **11**, 095001 (2022).
45. J. Lee, A. C. Silverman, E. Flitsiyan, M. Xian, F. Ren, and S. J. Pearton, "Impact of neutron irradiation on electronic carrier transport properties in Ga_2O_3 and comparison with proton irradiation effects." *Radiat. Eff. Defects Solids*, **178**, 680 (2023).
46. A. Y. Polyakov et al., *Physica B*, **376-377**, 523 (2006).
47. A. Y. Polyakov et al., *J. Appl. Phys.*, **100**, 093715 (2006).
48. A. Y. Polyakov, N. B. Smirnov, A. Govorkov, A. Markov, S. J. Pearton, N. Kolin, D. Merkurisov, V. Boiko, C. Lee, and I. H. Lee, *J. Vac. Sci. Technol.*, **B25**, 436 (2007).
49. S. Yue, X. Zheng, Y. Hong, X. Zhang, F. Zhang, Y. Wang, X. Ma, and Y. Hao, *IEEE Trans Electron Dev*, **70**, 3026 (2023).